



## Deformation of bitumen based porous material: Experimental and numerical analysis

Nadia Mokni<sup>a,\*</sup>, Sebastia Olivella<sup>a</sup>, Xiangling Li<sup>b</sup>, Steven Smets<sup>c</sup>, Elie Valcke<sup>c</sup>, An Mariën<sup>c</sup>

<sup>a</sup> Department of Geotechnical Engineering and Geosciences, Technical University of Catalunya, Jordi Girona, 1-3, (D2), 08034 Barcelona, Spain

<sup>b</sup> EIG EURIDICE, Boeretang 200, 2400 Mol, Belgium

<sup>c</sup> Waste and Disposal Expert Group, The Belgian Nuclear Research Centre, SCK-CEN, Mol, Belgium

### ARTICLE INFO

#### Article history:

Received 19 November 2009

Accepted 10 July 2010

### ABSTRACT

This paper presents a theoretical and experimental work aiming at understanding the mechanical behaviour of Bituminized Waste Product (BWP). This material is considered for this purpose as a mixture of bitumen and crystals of sodium nitrate. For BWP, both bitumen and crystals contribute to the creep deformations. In this study, an attempt is made to develop an elasto-viscoplastic model that describes the creep behaviour of BWP considering the constituents' creep behaviour.

An experimental program has been set up to get insight in the material response. The elasto-viscoplastic constitutive model has been implemented into a finite element program. The modelling results have been compared with the experimental data.

Crown Copyright © 2010 Published by Elsevier B.V. All rights reserved.

### 1. Introduction

Since the late 1960s, bitumen has been applied by the nuclear industry as a matrix for the immobilisation of low and intermediate level radioactive wastes, amongst others because of its good binding capacity, its low solubility and low permeability to water, and its good chemical and biological inertia. Depending upon the nature of the confined waste and in consequence to the chemical pre-treatment process, the bituminized waste contains important quantities of soluble salts.

The intermediate-level bituminized radioactive waste called Eurobitum has been produced at the EUROCHEMIC/BELGOPROCESS reprocessing facility (Mol-Dessel, Belgium), to immobilise precipitation sludge and evaporator concentrates originating from the chemical reprocessing of spent nuclear fuel and cleaning of high-level waste storage tanks. Eurobitum typically contains between 20% and 30% in weight of sodium nitrate ( $\text{NaNO}_3$ ) and about 60% in weight of hard bitumen Mexphalt R85/40. The remainder of the BWP consists of sparingly soluble salts such as  $\text{CaSO}_4$ ,  $\text{CaF}_2$ , and  $\text{Ca}_3(\text{PO}_4)_2$ , and oxides and hydroxides of Al, Fe, and Zr. Radionuclides are estimated to be present but for some 0.2 wt.% at most [1].

The current reference solution of the Belgian Agency for the Management of Radioactive Waste and Fissile Materials (OND-RAF/NIRAS) envisages the direct underground disposal of this waste in a geologically stable clay formation. In Belgium, the Boom Clay is studied as a potential host formation because of its favor-

able properties to limit and delay the migration of the leached radionuclides to the biosphere over extended periods of time.

Under geological disposal conditions the main factor that affects the long term behaviour of the material is water uptake, which is expected to take place at an extremely low rate given the low permeability of the waste and the surrounding multibarrier isolation systems. At the long term conditions, when the water reaches the waste, the hygroscopic soluble salts incorporated in the BWP (i.e.  $\text{NaNO}_3$ ) will take up ground water resulting in dissolution and subsequent leaching of these salts. The material progressively becomes porous and permeable, but the rate of this process is controlled by the mobility of the water and solute. Moreover, it is well known that porous materials containing salts may undergo swelling by water uptake induced by osmotic flows [2]. As mechanical effects are expected, it is necessary to investigate the deformation properties of this waste and its possible interaction with the multibarrier system, especially with the host rock.

For bitumen, creep deformations are expected and these depend in a nonlinear way on stresses and temperature [3,4]. In addition, several factors like chemical composition and structure of the bitumen, time, temperature, radiation and exposure to oxygen might induce a change of the rheological properties of bitumen with time (a phenomenon called ageing). As bitumen ages, it becomes harder and increasingly brittle [5]. When other viscoplastic constituents are introduced into it, the creep behaviour of the resulting multi-component material (mixture) may be influenced, as is the case of the BWP.

Another characteristic of the BWP is the presence of pores inside the bitumen matrix, which affect the creep behaviour, and which requires a specific numerical treatment when building the

\* Corresponding author.

E-mail address: [nadia.mokni@upc.edu](mailto:nadia.mokni@upc.edu) (N. Mokni).

constitutive law. A good understanding of the mechanical behaviour of the BWP is thus an absolute prerequisite for understanding the overall behaviour of such a complex mixture material. The objective here is to develop a model capable of predicting the overall creep strain of a mixture of bitumen and salt crystals. The model will be used later for the analysis of swelling tests in which the material is allowed to attract water in a short time period.

**2. Experimental aspects**

To investigate the mechanical behaviour of the BWP, two types of tests have been performed: (1) unconfined compression tests and (2) confined compression tests (oedometer tests).

**2.1. Unconfined compression creep tests**

The experiments are focused on the creep behaviour of the studied materials. Several bitumen/salt mixtures were tested [6]. Tests were also conducted on pure bitumen samples, for reference. The description of the samples is shown in Table 1.

The experimental set-up is shown in Fig. 1. The diameter of the sample was smaller than that of the cell, thus allowing lateral deformation (unconfined condition). The cell itself was put in the oedometer frame for application of the vertical stress. An oedometer frame is an apparatus to apply stress, by means of weights and a lever, on a cell that usually contains a confined porous sample. Different constant loading steps were applied on the samples. Each loading step was applied instantaneously and maintained for about 30 min. The vertical displacement for each loading step was recorded as a function of time. Meanwhile, the temperature inside

and outside the cell was carefully monitored in order to check its possible influence on the measurement. The results allow interpreting the creep behaviour of the bitumen and the mixtures (bitumen/salt) at various stress levels.

The result of the constant stress creep test is displayed in Fig. 2a. Here the steady state strain rate is plotted against the stress for six specimens. For reference, Fig. 2b shows the results obtained by Cheung and Cebon [3], which indicate that the creep of pure bitumen and the BWP can be represented by a power law equation relating strain rates with the power of the stress. Although the results show some scattering, it can be seen that the behaviour of the pure bitumen and the BWP can be represented by a creep power law, in a similar way as reported in the literature [3,4] for other bitumens. The incorporation of salt crystals decreases strain rates. This is expected as the crystals deform at slower rates as compared with bitumen material.

**2.2. Confined compression tests**

A confined compression test consists of a series of steps of uniaxial deformation under confined conditions, i.e. with lateral deformations not permitted. This test, often referred to as oedometer test, is quite standard in mechanics of porous materials, and it was originally developed in the field of soil mechanics. An oedometer test produces vertical deformations which imply volumetric deformations ( $\epsilon_{volumetric} = \epsilon_{vertical}$ ) and deviatoric deformations ( $\epsilon_{deviatoric} = (2/3)\epsilon_{vertical}$ ).

A series of confined compression tests was performed on non-radioactive samples taken from drums of Eurobitum produced about 25 years ago, during the inactive start-up phase of the bituminisation plant. The production method and composition of this non-radioactive reference BWP are entirely similar to that of the radioactive BWP, except for the presence of radionuclides. The samples had a diameter of 38 mm and were 10 mm in height, and were artificially aged before the tests (by gamma irradiation in the absence of oxygen) [5].

The tests were performed using a conventional oedometer cell, with sintered metal filters above and below the samples, so that the material could be hydrated in a later phase (water-uptake test) (Fig. 3). It is assumed that the samples were dry before the compression tests. However some condensed water could have reached the pores.

**Table 1**  
Description of samples tested.

No.	Reference	Descriptions
1	Mexphalt R85/40	Pure bitumen without salts
2		
3	BWP 0-2//CR15/16//08	Reference Eurobitum with 28 wt.% NaNO <sub>3</sub>
4	BWP 0-4//CR15/15//09	Reference Eurobitum with 28 wt.% NaNO <sub>3</sub>
5	BWP 0-3//CR15/9//08/18	Eurobitum with 18 wt.% NaNO <sub>3</sub>
6	Mexphalt R85/40	Pure bitumen without salts
7		

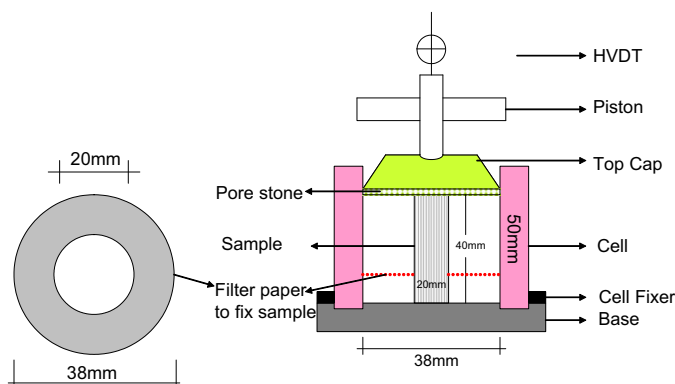


**Fig. 1.** Device for the unconfined compression test.

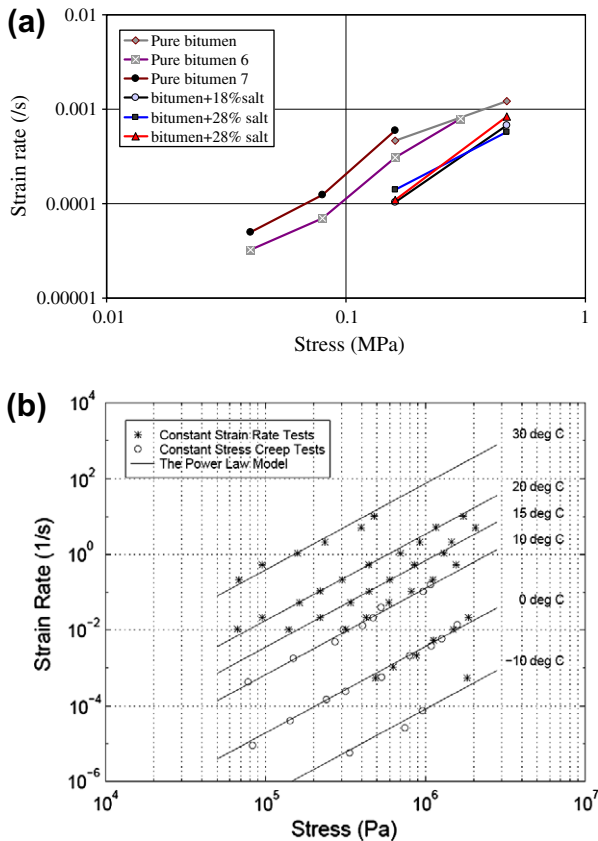


Fig. 2. (a) Steady state creep behaviour in compression for Eurobitumen. (b) Steady state creep behaviour of a different bitumen (Cheung and Cebon [3]).

A series of seven experiments was performed on non-radioactive BWP in a laboratory with controlled temperature (about 22 °C). The oedometric tests were performed under dry conditions. The tests mainly consist in the loading and unloading events which finally lead to a material which was practically incompressible (Fig. 4). Because the compression is irreversible, it is deduced that initial porosity is at least of the order of these irreversible deformations. In absence of porosity, the incompressibility of the material would not permit irreversible deformation under oedometric conditions. The soft nature of the bitumen permits to assume that porosity reduces during compression.

It has to be kept into consideration that this series of tests were performed in order to obtain mechanical properties of the studied materials. The stress level applied is close to the expected in situ stress conditions.

### 3. Mechanical constitutive model

The bituminized waste is considered as a homogeneous suspension of soluble NaNO<sub>3</sub> salt crystals in bitumen (Fig. 5a). As mentioned above, the hygroscopic soluble salts incorporated in the BWP will take up water from the surrounding host formation resulting in dissolution, but this is expected at a very low rate in geological disposal conditions. Therefore, the bitumen matrix progressively becomes porous and permeable. Fig. 5b shows the development of a porous layer at the surface of a sample exposed to water.

From a mechanical point of view, both bitumen and salt crystals show significant creep deformation that may control the response of the mixture. The complex mechanical behaviour of such a material requires an adequate mechanical constitutive model to describe its elastic and viscoplastic behaviour.

For a material presenting elastic-viscoplastic behaviour, the total strain tensor can be described by:

$$\varepsilon_{ij} = \varepsilon_{ij}^e + \varepsilon_{ij}^{vp} \quad (1)$$

where  $\varepsilon_{ij}^e$ ,  $\varepsilon_{ij}^{vp}$  denote the elastic and viscoplastic strain components, respectively.

#### 3.1. Constitutive model for creep deformation

In general the BWP can be envisaged as composed of a porous bituminized matrix embedding crystals (Fig. 6).

The total volume of the medium ( $V_t$ ) can be decomposed into the volume occupied by the crystals ( $V_c$ ), the pores (voids:  $V_v$ ) and the bitumen ( $V_b$ ), i.e.  $V_t = V_c + V_v + V_b$ . The volume of the pores varies as the consequence of dissolution of the crystals and may be occupied by water or air.

These volumes permit to define the volume fraction of the different components ( $\phi_c$  and  $\phi_b$ ) and the volume fraction of pores, i.e. the porosity ( $\phi$ ). These variables are defined as:

$$\phi_c = \frac{V_c}{V_t}; \quad \phi = \frac{V_v}{V_t}; \quad \phi_b = \frac{V_b}{V_t} \quad (2)$$

$$V_t = V_c + V_v + V_b; \quad 1 = \phi_c + \phi + \phi_b = \phi_c + \phi_m$$

$$\phi_m = \phi + \phi_b$$

The sum of the porosity ( $\phi$ ) plus the volume fraction of the bitumen ( $\phi_b$ ) is defined as the volume fraction of the porous bitumen matrix  $\phi_m$ , i.e.  $\phi_m = \phi + \phi_b$ .

In this way,  $1 - \phi_m = \phi_c$  is the volumetric fraction occupied by the crystals.

Creep of crystalline materials is modelled with the so-called creep power law [7], which relates deviatoric strain rates and deviatoric stresses, in a linear or nonlinear way. In addition, temperature effects and hardening or softening responses can be incorporated. Creep deformation of solids and viscous response of fluids are expressed with the same mathematical equation. In case of fluids it leads to Newtonian or non-Newtonian behaviour, respectively, for linear or nonlinear response. For Newtonian materials, the shear strain rate is proportional to the shear stress. The constant of proportionality is known as the viscosity. For non-Newtonian materials the linearity is lost and the strain rate is usually written as proportional to a nonlinear function of the shear stress.

Crushed rocks, metal powders and other porous materials like the porous bituminized matrix, made of viscous components, require constitutive equations with significant volumetric contribution as compared to crystals which are practically incompressible. Olivella and Gens [8] have developed a model for porous crushed salt that combines the power law and a simple geometric representation of grains and pores. The model has been applied to simulate an in situ test in the Asse salt mine performed during more than 10 years [10]. The crushed salt model converges to the model of rock salt as porosity vanishes. The fundamentals of the model developed by Olivella and Gens [8] are included in an Appendix. This model is used as the basis for the development of a model for the mixture of bitumen and crystals, both materials assumed to deform with elastic and creep contributions. A brief description of the model part that is used here has been included in an Appendix.

In the model presented here, the strain rates of a mixture can be obtained from the properties of the components under shear conditions assuming a weighted geometric average. This represents a combination of mechanisms in series and/or in parallel. Series would imply that the more deformable material dominates while parallel would imply that the stiffer material dominates. In contrast, the arithmetic average seems more appropriate for volumetric deformations, which represents more a combination of mecha-

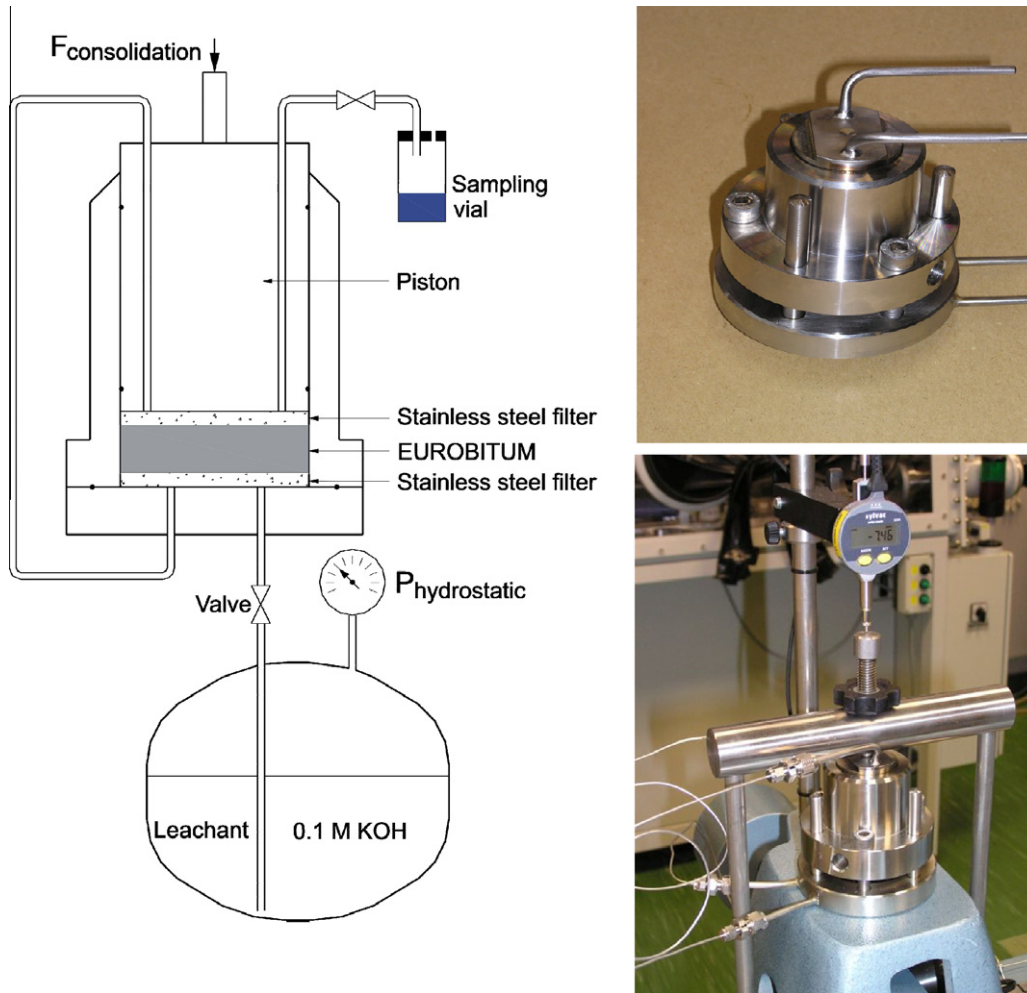


Fig. 3. Confined compression test set-up (combined with water-uptake test).

nisms in series in this case. Actually the crystals are more or less floating in the bitumen matrix. Under these assumptions, the viscoplastic strain of the mixture (BWP) would be defined as follows:

$$\begin{aligned} \frac{d\varepsilon_d^{vp}}{dt} &= \left(\frac{d\varepsilon_d^m}{dt}\right)^{\phi_m} \left(\frac{d\varepsilon_d^c}{dt}\right)^{\phi_c} \\ \frac{d\varepsilon_v^{vp}}{dt} &= \phi_m \left(\frac{d\varepsilon_v^m}{dt}\right) + \phi_c \left(\frac{d\varepsilon_v^c}{dt}\right) \end{aligned} \quad (3)$$

where  $\varepsilon^m$  and  $\varepsilon^c$  denote, respectively, the viscoplastic strain of the bitumen matrix and of the crystal, and the subscript “d” stands for deviatoric (shear) while the subscript “v” corresponds to volumetric. These assumptions imply that the crystals have more effect on deviatoric deformation than on volumetric. Other possibilities could be investigated. As will be shown below, assuming these combinations permits to obtain the form of the equivalent parameters for power and viscosity in a relatively simple way.

As explained above, the creep of crystalline materials is governed by a power law, so the following equation is considered for the crystals:

$$\frac{d\varepsilon_{ij}^c}{dt} = A_c q^{n_c} \frac{\partial q}{\partial \sigma_{ij}} \quad (4)$$

where  $A_c(T)$  is a temperature dependent parameter,  $n_c$  the power of the deviatoric stress of the creep law of the crystal, and  $q$  the deviatoric stress. It is important to notice that this law does not allow volumetric creep deformation.

The description of the mechanical behaviour of the porous bitumen matrix requires constitutive equations with significant volumetric creep contribution. As indicated above, Olivella and Gens [8] developed a model to represent the creep behaviour of porous salt aggregates. Creep for this kind of materials is explained with the theory of dislocations (Dislocation Creep deformation), which refers to intracrystalline mechanisms, and is characterized by a power law. In contrast, the bitumen used for the bituminized waste is an amorphous polymer material [3], but its creep can also be described with a power law in the range of stresses and temperatures considered in this research. So the common point is the creep power law, which is referred to also as a non-newtonian fluid equation. While crystalline rocks are solid materials, bitumen has a behaviour that is closer to that of fluids.

The mechanical model was based on an idealized geometry (polyhedrons representing the particles) that was used as a basis for calculating strain rates and to obtain macroscopic laws (see Appendix). It should be noticed that all geometrical variables were only a function of porosity (actually: void ratio). In that model, it was assumed that volumetric deformation was produced by the deviatoric deformation of the solid phase (example: a packing of incompressible spheres may reduce its porosity if the spheres change their shape).

Considering the adopted geometry and making further assumptions of stress distributions in the solid mass, the model was expressed in the following generalized form (see Appendix):

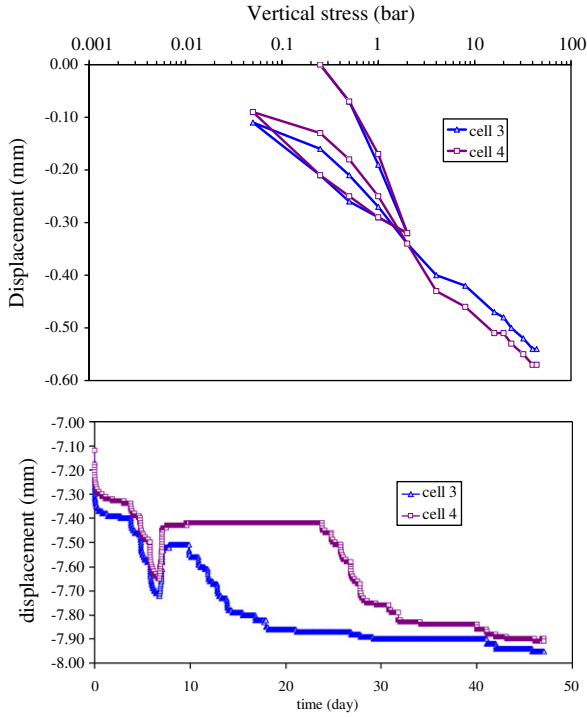


Fig. 4. Representative odometer test results (cell 3 and cell 4).

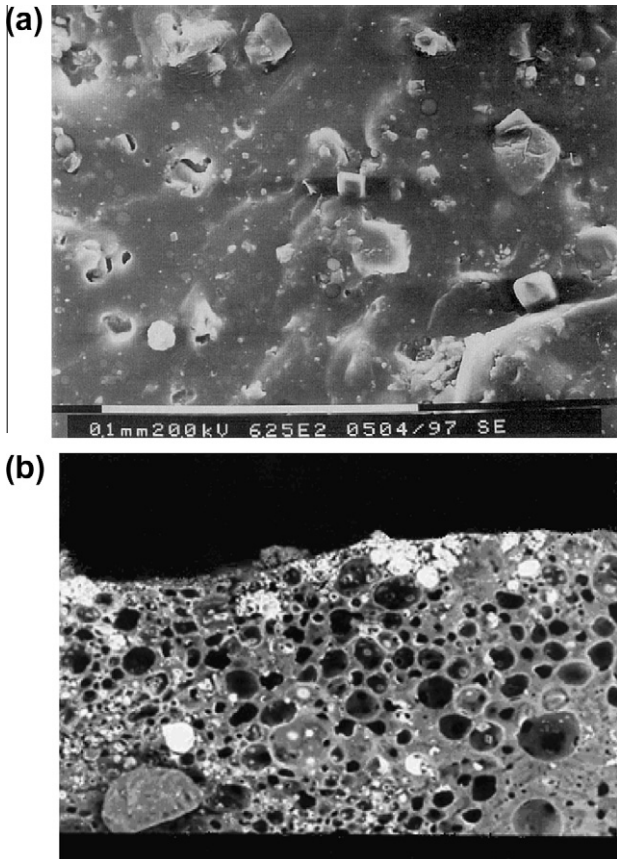


Fig. 5. ESEM observations of BWP: (a) observation of a dry sample of BWP after Kursten and Van Iseghem [12] and (b) observation of a leached synthetic BWP after Sercombe [9].

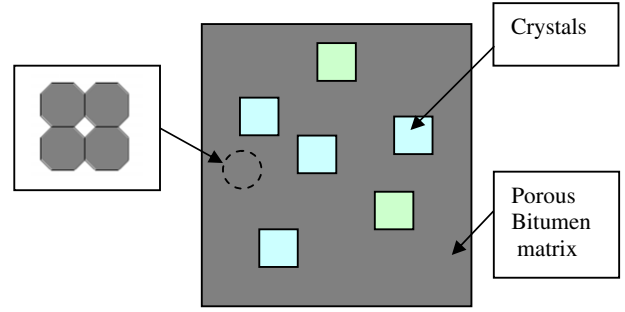


Fig. 6. Schematic representation of the medium.

$$\frac{d\varepsilon_{ij}^{vp}}{dt} = \frac{1}{\eta} \Phi(F) \frac{\partial G}{\partial \sigma'_{ij}} \quad (5)$$

where  $G$  is the viscoplastic potential to describe the flow rule,  $F$  is a stress function,  $\phi$  is a scalar function and  $\eta$  is a viscosity parameter. The application of the model to the bitumen matrix requires only the use of the appropriate material parameters  $A_m$  and  $n_m$  (see below).

Therefore, it is possible to write:

$$F = G = \sqrt{q^2 + \left(\frac{p}{\alpha_p}\right)^2}; \quad \Phi(F) = F^{n_m} \quad (6)$$

where  $\alpha_p$  was a function of viscosities, i.e.:

$$\eta = \eta^d, \quad \alpha_p = \left(\frac{\eta^v}{\eta^d}\right)^{1/(n_m+1)} \quad (7)$$

where  $\eta^v$  and  $\eta^d$  are, respectively, viscosities for volumetric and deviatoric creep, defined as:

$$\frac{1}{\eta^v} = A_m g^v(\phi); \quad \frac{1}{\eta^d} = A_m g^d(\phi) \quad (8)$$

where  $A_m(T)$  is a temperature dependent parameter and  $n_m$  is the power of the deviatoric stress of the creep law of the bitumen matrix. The definition of  $g^v$  and  $g^d$  is given in the Appendix. Both Eqs. (4) and (5) are Perzyna type equations [7], respectively, for pure deviatoric deformation (4) and for coupled deviatoric–volumetric deformation (5). A main assumption here is that a material obeying a creep power law and containing pores can be modelled with a similar approach, irrespective of its micro structure (crystalline or amorphous).

In order to extend this model to a mixture and to incorporate the contribution of the salt crystals, the equivalent parameters are defined in the following way:

$$\frac{1}{\eta_{eq}^d(\phi)} = A_{eq}^d(\phi) = (A_m g^d(\phi))^{\phi_m} (A_c g^d(0))^{\phi_c} = (A_m g^d(\phi))^{\phi_m} (A_c)^{\phi_c} \quad (9)$$

$$\frac{1}{\eta_{eq}^v(\phi)} = A_{eq}^v(\phi) = \phi_m A_m g^v(\phi) + \phi_c A_c g^v(0) = \phi_m A_m g^v(\phi)$$

$$n_{eq}(\phi) = n_m \phi_m + n_c \phi_c$$

The form comes from the proposed assumption given above (Eq. (3)) and provides some conditions that are described later. Without loss of generality other assumptions could be considered, but the ones chosen (arithmetic mean for volumetric and for the power, and geometric mean for deviatoric) are a conjecture.

In this model extension, it is assumed that the crystals do not have pores, this is why the functions corresponding to crystals have been written for zero porosity. Actually this is equivalent to:  $g^v(0) = 0$  and  $g^d(0) = 1$  (apply zero porosity or void ratio to equations in the Appendix). Therefore, the volumetric contribution is due solely to the bitumen matrix deformation.

Finally, the viscoplastic potential and the stress function are written as:

$$G = \sqrt{q^2 + \left(\frac{p}{\alpha_p}\right)^2} \text{ and } F = \sqrt{q^2 + \left(\frac{p^{n_m}}{\alpha_p}\right)^2} \text{ and } \Phi(F) = F^{n_{eq}} \quad (10)$$

$$\alpha_p = \left(\frac{\eta_{eq}^v(\phi)}{\eta_{eq}^d(\phi)}\right)^{\frac{1}{1+n_{eq}}} \quad \frac{1}{\eta_{eq}^v(\phi)} = A_{eq}^v(\phi) = \phi_m A_m g^v(\phi) \quad (11)$$

$$\eta = \eta_{eq}^d(\phi) \quad \frac{1}{\eta_{eq}^d(\phi)} = A_{eq}^d(\phi) = (A_m g^d(\phi))^{\phi_m} (A_c)^{\phi_c}$$

No threshold stress is defined, which implies that strain rates develop at any stress level (this is also the case for salt rock).

The new model was developed to accomplish the following conditions described below.

When the stress state is isotropic ( $(\sigma_1) = (\sigma_2) = (\sigma_3)$ ; the subscripts 1, 2, 3 indicate the principal stress directions) only the properties of the bitumen matrix play a role:

$$\frac{d\varepsilon_{ij}^{vp}}{dt} = \phi_m A_m g^v(\phi) p^{n_m} = \frac{1}{\eta_{eq}^v(\phi)} p^{n_m} \quad (12)$$

When pure shear conditions are reached ( $(\sigma_3) = -(\sigma_1)$  and  $(\sigma_2) = 0$ ) the equivalent parameters (power and viscosity) are recovered for the calculation of strains:

$$\frac{d\varepsilon_1^{vp}}{dt} = \frac{3}{2} A_{eq}^d(\sigma_1)^{n_{eq}} = \frac{3}{2} \frac{1}{\eta_{eq}^d(\phi)} (\sigma_1)^{n_{eq}} \quad (13)$$

Both viscosities  $\eta^v$  and  $\eta^d$  depend on the porosity (see Appendix). The shape of these functions is crucial to describe adequately the porosity influence on the creep deformations of the mixture. The chosen functions for viscosities have been represented in Fig. 7, considering the case of a porous bitumen matrix ( $\phi_c = 0$ ) and of a bituminised waste ( $\phi_c = 0.16$ ), and using  $n_{eq} = 2$ . It shows that  $\eta^v$  tends to infinity as porosity vanishes. Therefore, at low porosity the original power law (Eq. (4)) is recovered by Eq. (6). The limiting values can also be easily verified from Eq. (10):  $f$  tends to zero when the pore volume disappears (it tends to zero) and consequently  $g$  tends to 1. The effect of porosity on the volumetric creep is much larger than on the deviatoric creep, except for high porosities (close to 0.40). Fig. 7 also shows that changing the crystal volume fraction from 0 to 0.16 increases significantly the viscosity for deviatoric creep.

### 3.2. Elastic behaviour

Elastic volumetric deformations of the BWP are described by an appropriate nonlinear law which is a logarithmic relationship often found in constitutive models for soils.

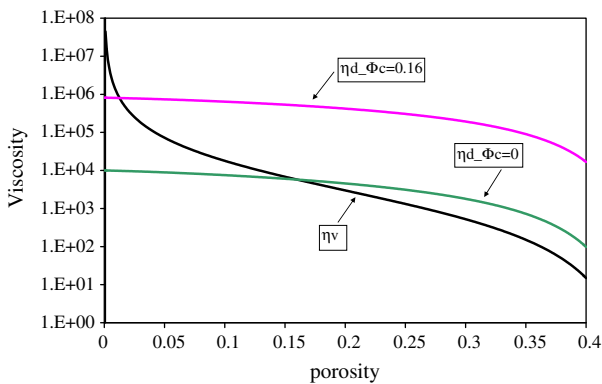


Fig. 7. Viscosities (in MPa<sup>2</sup> s) for volumetric and deviatoric creep as a function of porosity using  $n_{eq} = 2$ .

$$d\varepsilon_v^e = \frac{k}{1+e} \frac{dp'}{p'} = \frac{dp'}{K}; \quad K = \frac{p'(1+e)}{k} \quad (14)$$

where  $p'$  (MPa) is the mean effective stress (defined as  $p' = (\sigma_1 + \sigma_2 + \sigma_3)/3$ ),  $e$  and  $k$  are, respectively, the void ratio and the slope of the unload/reload curve in the  $(e - \ln p')$  diagram.  $K(p')$  is the nonlinear bulk modulus.

For a given initial stress, paths for which  $dp' > 0$  lead to compression and paths for which  $dp' < 0$  lead to expansion. Since the above defined logarithmic law does not allow tension, an additional condition is considered as follows:

$$K = \max\left(\frac{p'(1+e)}{k}; K_{min}\right) \quad (15)$$

In this equation,  $K_{min}$  is a lower bound of the stiffness modulus, which may be small but positive. It is used for low stress confinement and also for tension conditions.

### 3.3. General formulation for elasticity plus elasto-viscoplastic creep

In summary, a general formulation for elasticity plus creep (elasto-viscoplastic) law for the studied BWP can be written in the following way:

$$\frac{d\varepsilon_{ij}}{dt} = \frac{d\varepsilon_{ij}^{elastic}}{dt} + \frac{d\varepsilon_{ij}^{vp}}{dt} = \frac{d\varepsilon_{ij}^{elastic}(\sigma_{ij})}{dt} + \frac{d\varepsilon_{ij}^{vp}(\sigma_{ij}, T, \phi)}{dt} \quad (16)$$

which has a particular form for the isotropic case:

$$\frac{d\varepsilon_v}{dt} = a_1 \frac{1}{p'} \frac{dp'}{dt} + \frac{1}{\eta^v(T, \phi)} p^{n_m} \quad (17)$$

where  $a_1$  is a parameter for the nonlinear elastic contribution defined as:

$$a_1 = \frac{k}{1+e} \quad (18)$$

Although the isotropic part is used here for the description of the model equations, the model is used for a general stress state, including a Poisson ratio for the elastic part and the full viscoplastic formulation for the creep part as given above.

As it has been written above, the model does not allow extension behaviour. In that case, when the material is subjected to tension stresses, Eq. (17) becomes:

$$\frac{d\varepsilon_v}{dt} = \frac{1}{K_{min}} \frac{dp'}{dt} + \frac{1}{\eta^v(T, \phi)} |p'|^{(n_m-1)} p' \quad (19)$$

The described model includes thus nonlinear elasticity plus nonlinear creep. For elasticity the nonlinearity comes from the mean effective stress dependence of stiffness (Eq. (14)). The non-elastic part of the model is a power function of stress. As shown in Eq. (11) viscosity functions also depend in a nonlinear way of porosity.

## 4. Modelling of mechanical behaviour of BWP

The model described above has been implemented in the Finite Element code CODE\_BRIGHT. Several numerical simulations were performed in order to explore the model ability to reproduce the influence of the presence of the crystals on the creep behaviour of the BWP. A numerical exercise is first shown, which permits to consider assumptions to simplify the problem.

The numerical example concerns a simulation of a creep test under oedometric conditions (vertical stress = 0.2 MPa). The model parameters are summarized in Table 2. Fig. 8 displays the evolution of creep deformation with time for three cases: (1) porous bitumen matrix, (2) mixture of bitumen and 16% in volume of

**Table 2**  
Material parameters for the numerical example.

Parameters	Symbols	Values
Elastic model	$\nu$	0.3
	$a_1$	0.0078
Creep model	$n_m$	2.1
	$n_c$	5
Initial porosity	$\phi_0$	0.06

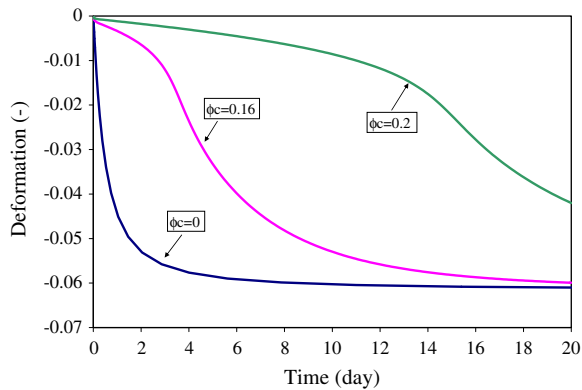


**Fig. 8.** Effect of crystal volume fraction on creep deformation for an oedometric test under constant vertical stress of 0.2 MPa.

NaNO<sub>3</sub> ( $\phi_c = 0.16$ ), and (3) mixture of bitumen and 20% in volume of NaNO<sub>3</sub> ( $\phi_c = 0.20$ ). The plot shows that creep deformations decrease significantly when  $\phi_c$  increases, at this stress level. This is a consequence of the increase of the viscosity for deviatoric creep.

#### 4.1. Modelling of compression tests under confined conditions

As explained in Section 2, a series of conventional oedometric tests with cylindrical inactive gamma irradiated Eurobitum samples containing 28% in weight of NaNO<sub>3</sub> were performed in the laboratory of SCK-CEN. From the experimental results it is clear that the material shows a nonlinear elastic behaviour (deformation varies rather linearly with the logarithmic vertical stress). These results permit to determine the parameters for the mechanical constitutive model described above in this paper.

An initial porosity of these samples for the oedometric tests was estimated to have the value  $\phi_0 = 0.06$  according to the deformation of the samples (a precise measurement would be envisaged). The parameters have been calibrated to simulate the experiment performed with cell 3 and cell 4 (Table 3), which are representative of the series of tests and show little scatter of the test results. The power of the creep power law for porous bitumen matrix has been deduced from the results of pure bitumen given in Fig. 2.

For the model prediction we have used the following values of the temperature dependent parameter of the bitumen matrix and the crystals:

**Table 3**  
Material parameters for modelling of compressions tests.

Parameters	Symbols	Values
Elastic model	$\nu$	0.3
	$a_1$	0.0078
Creep model	$n_m$	2.1
	$n_c$	5
Initial porosity	$\phi_0$	0.06
Crystal volume fraction	$\phi_c$	0.16

$$A_m(T) = 8 \exp\left(-\frac{22,900}{RT}\right) \quad (20)$$

$$A_c(T) = 5 \times 10^{-6} \exp\left(-\frac{59,650}{RT}\right)$$

It should be recalled that these viscosity parameters are not comparable as they correspond to power law creep equations with different power.

For the bitumen matrix, the constant inside the exponential has been taken from [3], while the pre-exponential constant has been determined to obtain a good prediction of the experimental test represented in Fig. 9. For the crystals, the adopted values correspond to typical values for rock salt deviatoric deformation [8]. Evolution of the deformation versus time for the oedometric cells together with the model results are shown in Fig. 9. The modelled results show many similarities with the experimental data (taking into account that the viscosity has been calibrated with these tests). They are characterized, for each loading step, by instantaneous deformations followed by creep. Beyond a certain time, for high stress levels volumetric creep deformations disappear because the volume of pores becomes negligible and the material shows only a volumetric elastic response.

It must be noticed that  $\eta^v$  tends to infinity as porosity vanishes, which guarantees that the volumetric creep part disappears progressively.

Some discrepancies are observed, however, between the experimental and model results. The model does not predict very well the large instantaneous deformations that occur immediately after the first loading. These discrepancies could be attributed to uncertainties that occurred during the experiment. In fact, it is unlikely that the piston was totally in contact with the sample after first

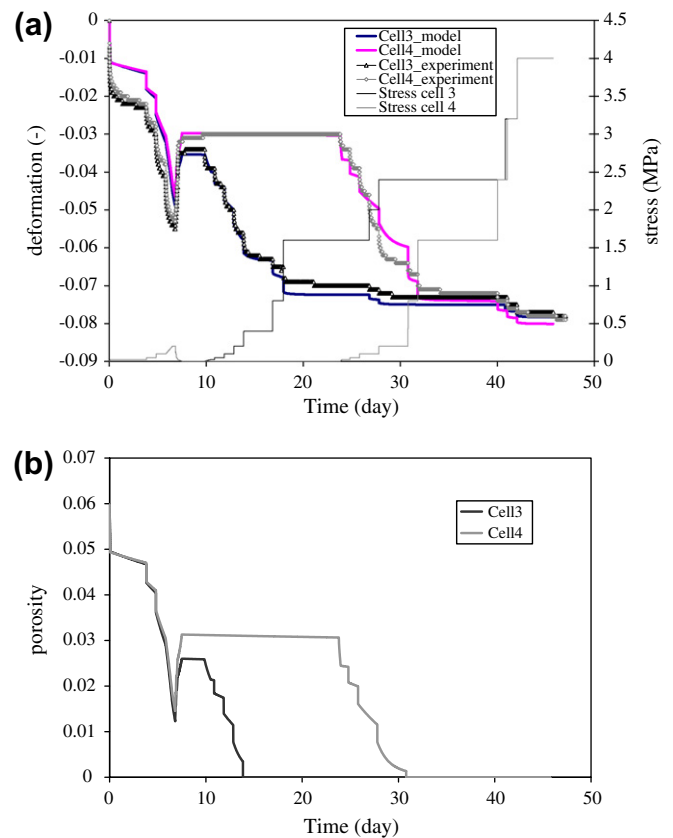


**Fig. 9.** Vertical deformations and porosity profile as a function of time for cell 3 and cell 4. Experimental results and model calculations. (a) Measured and calculated deformations and (b) porosity evolution during compression.

loading (25 kPa), since the upper surface of the material was rough. Therefore the first loading step produces a large deformation increment in the test which, as mentioned before, can be attributed to accommodation of the piston on the material surface. In contrast the model predicts the deformation increment corresponding to the first loading step (from 0 to 25 kPa).

**5. Simulation of other experiments under different conditions**

In Section 4, the model was applied to 2 experiments and the viscosity constant and elastic compressibility were calibrated.

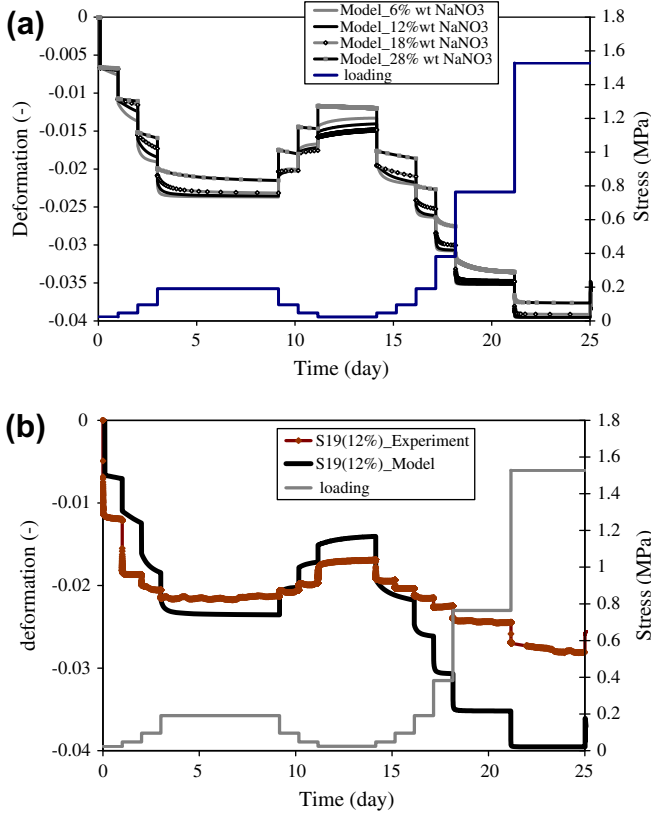


**Fig. 10.** Effect of crystal content in a multistep test (initial porosity 2.5%): (a) model results for different crystal contents (weight percent) and (b) comparison of model with experimental results for a test with 12% of salt content.

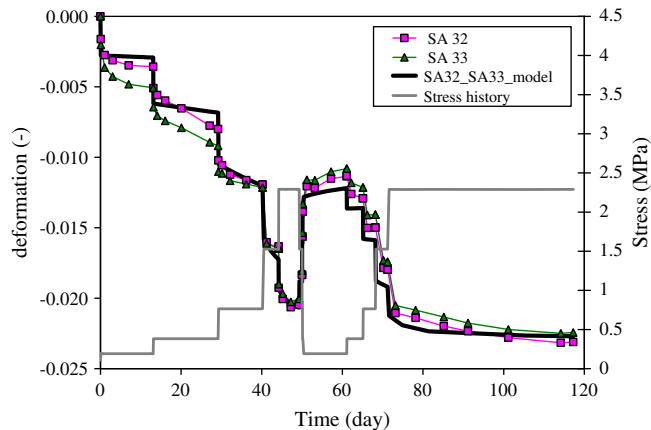


**Fig. 11.** Simulation of a test on a radioactive sample (initial porosity 2.5%, viscosity reduced by a factor of 1000).

The power of the creep law was maintained equal to the value determined from unconfined compression. In this section, other experiments are modelled. Fig. 10 shows the simulation of a multistep test under different conditions of crystal content and the comparison with experimental results. The sample in this case is assumed to have a low porosity (2.5%), as it was pre-compressed to guarantee good contact at the initial loading step. No variation of the model parameters has been carried out in this case. In addition, Fig. 11 shows the simulation of another multistep test for a radioactive sample. The radioactive BWP was of different nature as the material tested in experiments in Fig. 2: it was a less deformable material, and the viscosity constant (*A*) had to be reduced by a factor 1000 to simulate the test results (two series showing good repeatability).

Further experiments will be modelled in the future and special attention should be paid to the initial conditions of the material before application of the stress levels.

**6. Concluding remarks**

According to the present Belgian radioactive waste management program, Eurobitum bituminised radioactive waste will be disposed of in a geologically stable underground clay formation. The presence of the radioactive waste should not disturb the favorable properties of the host formation. The interaction of a BWP and the host formation is complex due to the presence of hygroscopic salts. To better understand the interaction between the swelling Eurobitum and the host formation, coupled hydro-chemical-mechanical constitutive laws have to be developed. An essential part of the modelling approach is its mechanical response which should be interpreted with a constitutive equation.

This paper presents the laboratory and numerical research on the mechanical behaviour of a BWP. The material is considered as a porous medium, i.e. a mixture of a porous bitumen matrix and salt crystals. A model that predicts the overall creep behaviour of the BWP, whose both constituents are viscoplastic, has been presented. The model has been included in a finite element program. The influence of the crystals on deviatoric creep deformation has been investigated. The results of the numerical test offer a preliminary evidence of the effect of the crystals on the creep deformation. It has been observed that there is a significant decrease of creep deformation when the crystal volume fraction increases. The creep model has been compared with the experimental data. It has been observed that by volumetric deformation the bituminized waste evolves from porous conditions to an incompressible material.

**Acknowledgments**

The work of the first author is funded by a research grant from ONDRAF/NIRAS, the Belgian Agency for the management of radioactive waste and fissile materials, as part of its programme on the geological disposal of high and medium level long-lived radioactive waste.

**Appendix A. Constitutive model for nonlinear creep of porous materials**

In this Appendix derivation of the model for creep of porous materials obeying power law developed in Olivella and Gens [8] is included.

The most common way to write the creep power law is:

$$\frac{d\varepsilon_{ij}}{dt} = Aq^n \frac{\partial q}{\partial \sigma_{ij}} \tag{A1}$$



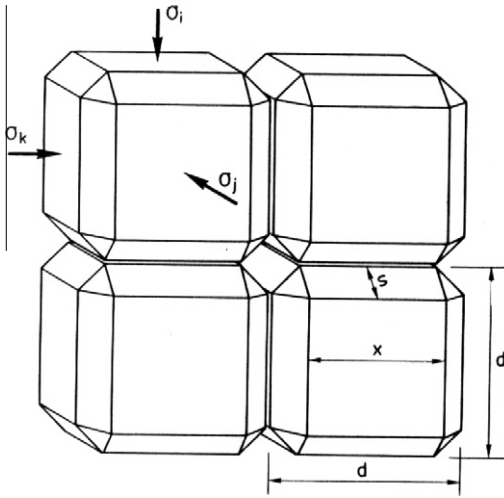
in the generalized case, ( $q = \sqrt{3J_2}$ ) refers to the deviatoric stress, ( $J_2$ ) is the second invariant of the deviatoric part of the stress tensor.  $A(T)$  is a temperature dependent parameter, and  $n$  is the power of the creep law. It is important to notice that this law does not allow volumetric creep deformation. This power law is combined with an idealized geometry to obtain a law for porous materials.

Yet, another form of the power law can be obtained if the generalized one is particularised for the principal directions ( $i$ ):

$$\frac{d\epsilon_i}{dt} = \frac{3}{2} A q^{n-1} (\sigma_i - p) \quad (A2)$$

where  $p$  refers to the mean stress. It does not matter if effective or total stress is used here because deviatoric stresses do not depend on pore pressure and this law does not contain volumetric contribution. Therefore, for porous materials, net stresses ( $\sigma'_{ij} = \sigma_{ij} - P_f \delta_{ij}$  in which  $P_f$  refers to the fluid pressure) will be considered in what follows. Assumptions are necessary to develop a macroscopic law, these are: simple stress distribution in the solid phase, the solid phase changes its shape without volume change, creep power law is valid to calculate the creep deformation of the solid phase. The macroscopic equations of the model will be built in three steps: (1) adoption of a stress distribution in a grain, (2) calculation of strain rates along the principal directions, and (3) generalization of the model to a tensorial form.

A simplified geometry for solid phase and pores was considered with the following derived functions:



Porosity ( $\phi$ ) and void ratio ( $e$ ) are two different ways to measure the void volume in porous materials. While porosity is the void volume divided by the total volume, the void ratio is the void volume divided by the solid volume. They are related by:  $e = \frac{\phi}{1-\phi}$  and  $\phi = \frac{e}{1+e}$ . Therefore the model can be written in terms of void ratio or porosity without loss of generality.

For the geometry of polyhedrons adopted, a simplified stress distribution inside the solid phase was considered:  $(\sigma'_i)_c = (\sigma'_i)(d^2/x^2)$  which simply establishes that the stresses in the contact increase as the area of the contact decreases. Considering the principal directions normal to the faces of the solid phase volumetric element, the strain rate for each principal direction can be calculated:

$$\frac{d\epsilon_i}{dt} = \left( \frac{1}{d} \frac{dd}{dt} \right)_i \cong \frac{3}{2} A q_i^{n-1} ((\sigma'_i)_c - p_i) \frac{\sqrt{2}s}{d} + \frac{3}{2} A q_i^{n-1} (\sigma'_i - p') \frac{x}{d} \quad (A3)$$

where  $p'_i$  and  $q_i$  are mean net stress and deviatoric stress in the zone of the solid phase near to the contact, i.e. computed with,  $(\sigma'_i)_c$ ,

$(\sigma'_j)_c$  and  $(\sigma'_k)_c$ ; while,  $p'$  and  $q$  are mean net stress and deviatoric stress in the internal zone of the solid phase, i.e. computed with  $(\sigma'_i)$ ,  $(\sigma'_j)$  and  $(\sigma'_k)$ . In this equation, the first term corresponds to the strain of the area near contacts and the second term corresponds to the strain in the core of the solid phase. As porosity tends to zero, the first term vanishes, and the original creep power law is obtained. A simple relationship is obtained if the stress state is considered isotropic, i.e.  $(\sigma'_1) = (\sigma'_2) = (\sigma'_3)$ :

$$\begin{aligned} \frac{d\epsilon_v}{dt} &= \frac{d\epsilon_1}{dt} + \frac{d\epsilon_2}{dt} + \frac{d\epsilon_3}{dt} = 3A((p')_c - p')^n \frac{\sqrt{2}s}{d} \\ &= 3A \left( \frac{(1+e)}{(\sqrt{1+e} - \sqrt{2e/\lambda_v})^2} - 1 \right)^n \frac{\sqrt{2e/\lambda_v}}{\sqrt{1+e}} (p')^n \\ &= \frac{1}{\eta_v^{bc}(e, T)} (p')^n \end{aligned} \quad (A4)$$

As an opposite state to isotropic, pure shear stress state is considered, i.e.  $(\sigma'_3) = -(\sigma'_1)$  and  $(\sigma'_2) = 0$ :

$$\frac{d\epsilon_1}{dt} = \frac{3}{2} A(T) \left( (\sqrt{1+g+g^2})^{n-1} \left( \frac{2g+1}{3} \right) f + (\sqrt{3})^{n-1} \frac{1}{\sqrt{g}} \right) \sigma_1^n \quad (A5)$$

The reason for these two particularizations (isotropic and pure shear) is to obtain simple relationships for volumetric strain rate and deviatoric strain rate. If a general stress state was assumed without any restrictions, these forms would be more complex due to the nonlinear (power) dependence of strain rate on stress for this mechanism. From (A4) and (A5) the following viscosities for volumetric and deviatoric creep can be obtained:

$$\frac{1}{\eta^v} = A(T) g^v(e) \quad (A6)$$

$$\frac{1}{\eta^d} = A(T) g^d(e)$$

where

$$g^v(e) = 3(g-1)^n f \quad (A7)$$

$$g^d(e) = \left( \sqrt{\frac{1+g+g^2}{3}} \right)^{n-1} \left( \frac{2g+1}{3} \right) f + \frac{1}{\sqrt{g}}$$

$$g = \frac{1}{(1-f)^2} = \frac{d^2}{x^2} f = \sqrt{\frac{2e}{3(1-e^{3/2})(1+e)}} = \frac{s\sqrt{2}}{d} \quad (A8)$$

$A(T)$  and  $n$  come directly from the creep power law, i.e. the non-porous material. The functions  $g^v(e)$  and  $g^d(e)$  depend on the idealized geometry and in turn on void ratio. However, because the creep law has a power, a dependence on  $n$  remains in these functions.

Eq. (A3) has been developed on the basis of the idealized geometry adopted. However, it lacks generality because it has been written for strain rates along principal directions. One way to generalize (A3) is to use a flow rule. In this procedure, (A4) and (A5) are very useful to identify how this generalized form should be. The following general form, based on viscoplasticity theories for geological materials [11], was proposed:

$$\frac{d\epsilon_{ij}}{dt} = \frac{1}{\eta} \Phi(F) \frac{\partial G}{\partial \sigma'_{ij}} \quad (A9)$$

In this equation, a viscosity parameter is included,  $G$  is a viscoplastic potential,  $F$  is a stress function and  $\phi$  is a scalar function of  $F$ .

In Eq. (A9) the functions  $G$  and  $F$  should be taken as functions of stress invariants. The following form was proposed:

$$F = G = \sqrt{q^2 + \left(\frac{p}{\alpha_p}\right)^2} \quad (\text{A10})$$

$$\Phi(F) = F^n$$

where  $n$  is the power of the creep law and  $\alpha_p$  is a material function. Since  $\phi(F)$  is always positive, no threshold is considered in this law. This is consistent because creep materials develop viscous deformations under any stress level.

In order to exploit the theoretically derived Eqs. (A4)–(A8) this generalization of the model is complemented with definitions for  $\eta$  and  $\alpha_p$ . By comparison of A4 and A5 with the results obtained using A9 and A10 under the same stress state (i.e. isotropic and pure shear) it is obtained that:

$$\eta = \eta^d \quad \alpha_p = \left(\frac{\eta^v}{\eta^d}\right)^{\frac{1}{n+1}} \quad (\text{A11})$$

when void ratio (or equivalently porosity) vanishes  $\alpha_p$  tends to infinity and the volumetric term disappears.

## References

- [1] E. Valcke, A. Mariën, M. Van Geet, The methodology followed in Belgium to investigate the compatibility with geological disposal of Eurobitum bituminized intermediate-level radioactive waste, in: Mater. Soc. Symp. Proc. vol. 1193, 2009, pp. 105–116.
- [2] N. Mokni, S. Olivella, X. Li, S. Smets, E. Valcke, J. Phys. Chem. Earth (2008), doi:10.1016/j.pce.2008.10.008.
- [3] C.Y. Cheung, D. Cebon, J. Rheol. 41 (1996) 45–73.
- [4] C.Y. Cheung, D. Cebon, ASCE J. Mater. Civil. Eng. (1997) 117–129.
- [5] E. Valcke, F. Rorif, S. Smets, J. Nucl. Mater. 393 (2009) 175–185.
- [6] Yongfeng Deng, Anh-Minh Tang, Yu-Jun Cui, A study on the creep behavior of bitumen using unconfined compression test, Final test report, UR Navier/CERMES, Ecole des Ponts – ParisTech, 2009.
- [7] P. Perzyna, Adv. Appl. Mech. 9 (1966) 346–377.
- [8] S. Olivella, A. Gens, Int. J. Numer. Anal. Mater. Geom. 26 (2002) 719–746.
- [9] J. Sercombe, B. Gwinner, C. Tiffreau, B. Simondi-Teisseire, F. Adenot, J. Nucl. Mater. 349 (2006) 96–106.
- [10] S. Olivella, M. Luna, A. Gens, Thermo-mechanical analyses of a large scale heating test in salt rock, in: E. Oñate, D.R.J. Owen, (Eds.), VII International Conference on Computational Plasticity, COMPLAS VII, CIMNE, Barcelona, 2003.
- [11] C.S. Desai, D. Zhang, Int. J. Numer. Anal. Methods Geomech. 11 (1987) 603–620.
- [12] B. Kursten, P. Van Iseghem, In situ corrosion experiments, Final report for 1995–1996, SCK-CEN-R-3247, SCK-CEN, Mol, Belgium, 1998.